Received: 6 November 2017 | Revised: 23 January 2018 | Accepted: 5 April 2018

DOI: 10.1002/pca.2771

RESEARCH ARTICLE

WILEY Phytochemical Analysis

UPLC-ESI-QTOF-MS^2 characterisation of *Cola nitida* resin fractions with inhibitory effects on NO and TNF-α released by LPS-activated J774 macrophage and on *Trypanosoma cruzi* and *Leishmania amazonensis*

Larissa Frankenberger[1] | **Tamara D. Mora**[2] | **Carolina D. de Siqueira**[2] | **Fabiola B. Filippin-Monteiro**[2] | **Milene H. de Moraes**[3] | **Maique W. Biavatti**[1] | **Mario Steindel**[3] | **Louis P. Sandjo**[1]

[1] Department of Pharmaceutical Sciences, CCS, Universidade Federal de Santa Catarina, Florianópolis, SC, Brazil

[2] Department of Clinical Analysis, Universidade Federal de Santa Catarina, Florianópolis, SC, Brazil

[3] Department of Microbiology, Immunology and Parasitology, Universidade Federal de Santa Catarina, Florianópolis, SC, Brazil

Correspondence
Louis P. Sandjo, Department of Pharmaceutical Sciences, CCS, Universidade Federal de Santa Catarina, 88040-900, Florianópolis, SC, Brazil.
Email: p.l.sandjo@ufsc.br

Funding information
CAPES (Coordenação de Aperfeiçoamento de Pessoal de Nível Superior); CNPq (Conselho Nacional de Desenvolvimento Científico e Tecnológico)

Abstract

Introduction: The resin of *Cola nitida* is used in western Cameroon as incense for spiritual protection and during ritual ceremonies. This plant secretion has never been investigated although previous chemical and biological studies on other resins have drawn many attentions.

Objective: The resin fractions which revealed inhibitory effect on nitric oxide (NO) and tumour necrosis factor alpha (TNF-α) released by lipopolysaccharide (LPS)-activated J774 macrophage as well as on intracellular forms of *Leishmania amazonensis* and *Trypanosoma cruzi* amastigote were chemically characterised. Moreover, their antiparasitic activities were compared to those of semi-synthetic triterpenes.

Methodology: The anti-inflammatory activity was evaluated by measuring the nitrite production and the TNF-α concentration in the supernatants of LPS-activated macrophages by antigen capture enzyme-linked immunosorbent assay. Moreover, the antiparasitic assay was performed by infecting the host cells (THP-1) in a ratio parasite/cell 10:1 (*L. amazonensis*) and 2:1 (*T. cruzi*) and then exposed to the samples. The resin was separated *in vacuo* by liquid chromatography because of its sticky behaviour and the chemical profiles of the obtained fractions (F1–F4) were established by dereplication based on UPLC-ESI-MS^2 data while semi-synthetic triterpenes were prepared from α-amyrin by oxidation reactions.

Results: Fractions F1–F4 inhibited NO and TNF-α almost similarly. However, only F1, F3 and F4 showed promising antiparasitic activities while F2 was moderately active against both parasites. Hence, F1–F4 were exclusively composed of pentacyclic triterpenes bearing oleanane and ursane skeletons. Semi-synthetic compounds revealed no to moderate antiparasitic activity compared to the fractions.

Conclusion: Although it will be difficult to prove the interaction resin-spirit, interesting bioactivities were found in the resin fractions.

KEYWORDS

antiprotozoal activity, *Cola nitida* resin, NO and TNF-α inhibition, pentacyclic triterpenes, UPLC-ESI-QTOF-MS^2

1 | INTRODUCTION

Looking back to my childhood (L.P.S) and based on souvenirs, people from the west region of Cameroon used and are still using dried resin from the *Cola nitida* tree (Sterculiaceae) as incense for spiritual protection and during ritual ceremonies. However, resins in the ancient centuries had many applications such as varnishes, adhesives, incense in churches, and for mummification.[1,2] This sticky solid played a particular role in the mummification process, due to the polymerisation of its constituents, essentially the lipophilic that protected body tissues from microbial attacks.[3] With the evolution of sciences, investigations revealed that resins are also full of small antimicrobial molecules.[3] These findings match the chemo-ecological interactions observed between resins plants producer and their environment. So, various studies reported that resins are produced by the plant tissues as a defensive tool to fight insect's evasion or as a defence mechanism against pathogenic infections.[4,5] Moreover, resin chemistry unveiled this secretion as a great source of secondary metabolites where the most identified are terpenoids, aromatics, fatty acids and terpenoic acids[6] endowed with interesting biological activities. Compounds identified from resins proved to be anti-inflammatory, antitumoral, antimicrobial, and larvicidal among others bioactivities.[2,6]

Cola nitida (Sterculiaceae) is a well known tree because of the caffeine high concentration in its nuts, which are largely consumed in sub-Saharan localities to counteract hunger, thirst, and tiredness.[7] As far as we know, the resin from *C. nitida* has never been investigated neither chemically nor biologically.

Since our research is dedicated to the search of new anti-inflammatory and antiparasitic entities, the resin fractions were assayed for their nitric oxide (NO) and tumour necrosis factor alpha (TNF-α) inhibition effect as well as for their anti-protozoal activity on intracellular forms of *L. amazonensis* and *T. cruzi* amastigote. The obtained activity prompted us to establish the fractions UPLC-ESI-MS^2 chemical profile. This hyphenated technique allows simultaneous identification of constituents in an organic mixture. Furthermore, it also permits to avoid routine phytochemical studies that can lead to known and well-investigated compounds. As performing the dereplication, it turned out that pentacyclic triterpenes were predominant in the resin supporting the observed anti-inflammatory activity. Previous studies intensively reported triterpenes as inhibitors of interleukin production. Moreover, these metabolites can also suppress in activated macrophages, the release of NO, TNF-α, interleukin 1 beta (IL-1β) and interleukin 6 (IL-6) which by consequence lead to the decrease of the biosynthesis and/or the release of cytokines from target cells that results in a less aggressive inflammatory response.[8-11]

2 | EXPERIMENTS

2.1 | Chemicals and materials

Acetonitrile (HPLC grade), methanol, and formic acid were purchased from Tedia (São Paulo, Brazil). Milli-Q system (18.2 MΩ, Millipore, Simplipak, France) was used to produce ultrapure water. All samples were filtered by syringe filters (13 mm, 0.22 μm, Analítica, Brazil). NMR data were recorded in an Ultrashield 300 MHz Bruker machine.

2.2 | Material collection and preparation of the resin fractions

The resin (2 g) was collected from the trunk of *C. nitida* in Bangoua, located at the western province of Cameroon with longitude 10°29′, and latitude 5°12′ as geographic coordinates.

The resin (1 g) was poured onto dichloromethane/methanol (1:1, *v/v*), sonicated, mixed with silica gel and dried on a rotary evaporator. The mixture was fractionated on a silica vacuum liquid chromatography (VLC) column using hexane, dichloromethane, ethyl acetate, and methanol as mobile phases. Fractions F1–F4 were obtained after solvent evaporation as follows: F1 (300 mg), F2 (300 mg), F3 (150 mg) and F4 (200 mg). A portion (1 mg) of each fraction was dissolved in acetonitrile/methanol 2:1 (5 mL) and filtered with a syringe filter to afford 200 μg/mL for fractions F1–F4.

2.3 | Biological assays

2.3.1 | Cell culture

The murine macrophage cell line J774 was maintained in DMEM (Dulbecco's Modified Eagle's medium) supplemented with 10% fetal bovine serum (FBS) containing 100 U/mL of penicillin, 100 μg/mL of streptomycin and 10 mM of 4-(2-hydroxyethyl)-1-piperazineethanesulfonic acid (HEPES). Cells were cultured at 37°C in an atmosphere of 5% CO_2 and the medium was changed every 48 h. The cells were cultured up to confluence 80–90% and then subcultured after dissociation by scraping using a rubber policeman.

2.3.2 | Cytotoxicity of the resin fractions on J774 macrophage cell line

To evaluate the cytotoxicity of the fractions, resazurin-based cytotoxicity assay (Alamar blue®) was performed.[12] For macrophages, 3×10^5 cells/well were seeded in DMEM supplemented with 10% FBS. After 24 h, the medium was replaced with medium containing the fractions at the concentrations 1, 2.5, 5, 10, 25, 50 and 100 μg/mL and incubated at 37°C for 24 h. Subsequently, cells were incubated with 100 μL (0.1 mg/mL) of resazurin dye for 3 h at 37°C. The fluorescence was measured at 1 h intervals using a microplate reader (IS55, Perkin Elmer, Waltham, MA) at 530–590 nm. Non-linear regression of each fraction versus cell viability in percentage was performed in order to obtain the toxicity concentration of 10% (concentration causing 90% cell viability) using *GraphPad Prism 5.0* (GraphPad Software 5.0, Inc., San Diego, CA).

2.4 | *In vitro* anti-inflammatory activity

The anti-inflammatory activity was performed with modifications of the protocol previously described by Herath et al.[13] Thus, the evaluation consisted by measuring the nitrite production using an indicator of NO synthesis in the supernatants of LPS-activated macrophages. A quantity of cells (2×10^5 cells/well) was seeded in a 24-well plate and after 24 h, the medium was changed and CC_{10} of each fraction

was added in DMEM supplemented with 10% FBS. After 15 min, the macrophages were stimulated with lipopolysaccharide (LPS) 10 μg/mL and incubated for 24 h. Subsequently, the supernatants were collected and the nitrite production was measured by adding 100 μL of Griess reagent[14] (1% sulfanilamide and 0.1% *N*-(1-naphthyl)ethylenediamine in 0.5% phosphoric acid). The absorbance was determined with a microplate reader (ELX800, BioTek, Winooski, VT) at 540 nm. Furthermore, the TNF-α concentration was determined by antigen capture enzyme-linked immunosorbent assay (ELISA) (BD Bioscience, San Jose, CA) according to the manufacturer's instructions.

2.5 | Statistical analysis

Results were shown as the mean ± standard deviation (SD) of three experiments. One-way analysis of variance followed by Dunnett's multiple comparisons test was performed, and the level of significance was set at $p < 0.05$ (GraphPad Software 5.0, Inc., San Diego, CA).

2.6 | *In vitro* antitrypanosomal and antileishmanial activities

Human macrophage cell line THP-1 (ATCC TIB202) was grown in RPMI-1640 without phenol red (Sigma-Aldrich, St Louis, MO), supplemented with 10% FBS (Life Technologies, Carlsbad, CA), 12.5 mM HEPES, penicillin (100 U/mL), streptomycin (100 μg/mL) and Glutamax (2 mM), at 37°C in a 5% CO_2 incubator. *Leishmania amazonensis* MHOM/BR/77/LTB0016 promastigotes, expressing β-galactosidase, were grown at 26°C in Schneider's insect medium (Sigma Chemical Co., St Louis, MO) supplemented with 5% heat inactivated FBS and 2% of human urine.

THP-1 cells (4.0×10^4 per well) were cultivated in 96-well plates in RPMI-1640 medium and incubated with 100 ng/mL of phorbol 12-myristate 13-acetate (PMA) (Sigma Chemical Co.) for 72 h at 37°C in a 5% CO_2, to allow THP-1 cells differentiation into non-dividing macrophages.[15] Four days-old culture promastigotes (4.0×10^6 parasites/mL) were washed with phosphate buffered saline (PBS), pH 7.4, and incubated in RPMI-1640 supplemented with 10% heat-inactivated human B+ serum for 1 h at 34°C for parasite opsonisation. THP-1 cells were incubated with a parasite/cell ratio of 10:1 for 4 h at 34°C and 5% CO_2. After this period non-adherent parasite were removed by one wash with PBS and infected cells were incubated with 180 μL of full supplemented RPMI-1640 medium for another 24 h to allow the transformation of promastigotes into intracellular amastigotes.

The β-galactosidase *T. cruzi*, Tulahuén strain was provided by the Laboratory of Cellular and Molecular Parasitology, Centro de Pesquisas René Rachou, FIOCRUZ, Belo Horizonte. Culture-derived typomastigotes raised from infected L929 cell line were used to infect differentiated THP-1 (4.0×10^4 cells/well) in 96-well microplates in a parasite/cell ratio of 2:1 and incubated overnight at 37°C in a 5% CO_2 atmosphere. The medium containing non-internalised parasites was removed and replaced with 180 μL of fresh medium.[16]

Samples were solubilised in dimethyl sulfoxide (DMSO) and serially diluted (500 μg/mL to 2 μg/mL). Infected cells monolayer was treated by addition of 20 μL of each sample, in triplicate, followed by incubation for 48 h at 34°C or 37°C, 5% CO_2. After treatment, cells were carefully washed with PBS and incubated for 16 h at 37°C with 250 μL of chlorophenol red-ß-D-galactopyranoside (CPRG) (Sigma-Aldrich Co.) at 100 μM and Nonidet P-40 (NP-40) (Amresco Inc, Solon, OH) 0.1%. Optical density was read at 570/630 nm in an Infinite M200 (Tecan, Grödig, Austria).[17,18] The concentration of each sample that reduced parasite viability by 50% when compared to untreated control (IC_{50}) was estimated by non-linear regression of concentration-response curves. Amphotericin B (Sigma-Aldrich) and benznidazole (Sigma-Aldrich) were used as positive control for antileishmanial and antitrypanosomal activities, respectively, and DMSO 1% as negative control. The concentration capable to inhibit 50% (IC_{50}) of the parasites and the proliferation of THP-1 cells (CC_{50}) were used to express the antiparasitic activity and cytotoxicity, respectively. Selectivity index (SI) of each sample was determined by the ratio of CC_{50}/IC_{50}.

2.7 | Cell viability assay (MTT)

THP-1 cells were grown and cultivated in 96 well plates (4.0×10^4 cells/well) and treated with the compounds serially diluted in concentrations ranging from 2 μg/mL to 500 μg/mL and incubated for 72 h at 37°C, 5% CO_2. The plates were centrifuged (3.700 ×g/7 min), the supernatant was removed, and the cells were resuspended in 50 μL of a solution of MTT (Amresco) at 3 mg/mL in saline buffer and incubated for 4 h at 37°C, 5% CO_2 and centrifuged (3.700 ×g/7 min) and the formazan salt was solubilised in 100 μL DMSO. Optical density was determined at 540 nm in a Tecan® Infinite M200 spectrophotometer. DMSO 1% (*v*/*v*) and DMSO 50% (*v*/*v*) were the negative and positive controls, respectively. The IC_{50} values were calculated by a non-linear regression using the GraphPad Prism program.[15]

2.8 | UPLC–MS analysis

Chromatographic separations were carried out on an Acquity UPLC system class H (Waters, Milford, MA) equipped with a photodiode array (PDA) detector, sample manager and a quaternary solvent manager as well as a BEH C18 column: 50 mm, 1.0 mm, particle size 1.7 μm (Waters). Temperatures of the column and the samples tray were 40°C and 20°C, respectively. A volume of 3 μL was injected in a gradient condition at flow rate of 0.3 mL/min: 90% A (water/formic acid, 99.9/0.1 (*v*/*v*)) and 10% B (acetonitrile); 1–2 min, 90% of A; 2–10 min, 55% of A; 10–15 min, 10% of A; 15–20 min, 90% of A.

Mass data were recorded on a Xevo G2-S QTof (Waters) with an electrospray ionisation (ESI) probe operating in positive and negative ionisation modes. Nebuliser gas: nitrogen; cone gas flow 60 L/h; desolvation gas flow 900 L/h; sampling cone 40 V; source offset 80 V; collision gas: argon; Lockspray reference sample was Leucine encephalin with reference masses at *m*/*z* 556.2771 (ESI+) and m/z 554.2615 (ESI−). Temperatures of desolvation and of the ionisation source were 300°C and 120°C, respectively, while the capillary voltage was 3 kV. Collision energy was 30 eV. Data were acquired in a range of 100–1500 Da, at a scan time of 1.0 s during 20 min, and were processed with MassLynx V4.1 (Waters).

2.9 | Isolation of α-amyrin and chemical modification

Recrystallisation procedure using different solvents was performed with F1–F4. The mixture of α- and β-amyrin (60 mg) was obtained from F4 while the others did not provide any precipitation. A chromatographic column on silica gel using hexane and dichloromethane in gradient condition provided α-amyrin (48 mg) and the mixture of both metabolites (9 mg). Their structure was confirmed by NMR data in conjunction with those reported in the literature. α-Amyrin (15 mg) was subjected to different oxidation reactions using three different conditions: (1) pyridinium chlorochromate (PCC, 2 equivalents) and silica gel (5 mg) in dichloromethane at room temperature for 1 h; (2). $KMnO_4$/$KClO_3$ (2 equivalents each) in dichloromethane/acetone/water (5:5:1, 11 mL), at room temperature for 20 h; (3) potassium permanganate ($KMnO_4$)/potassium chlorate ($KClO_3$)/PCC (2 equivalents each) in dichloromethane/acetone/water (5:5:1, 11 mL), at room temperature for 20 h. Three triterpenes related to α-amyrin namely α-amyrone, 11-oxo-α-amyrin, and 11-oxo-α-amyrone were obtained after VLC purification in 70, 10, and 15% yield, respectively. The purification was performed with hexane and ethyl acetate in a gradient condition. Their structure was established by NMR data (Supporting Information Figures S1–S4) in comparison to those reported in the literature.

3 | RESULTS

The sticky behaviour of *C. nitida* resin prompted us to perform VLC using hexane (F1), dichloromethane (F2), ethyl acetate (F3) and methanol (F4). Since no previous studies were found on this organic material, the fractions were further investigated for their anti-inflammatory as NO and TNF-α inhibitors. In addition, F1–F4 were also investigated for their antiparasitic activities against the intracellular amastigotes of *L. amazonensis* and *T. cruzi*.

3.1 | Biological activity

3.1.1 | Anti-inflammatory activity

In order to evaluate the anti-inflammatory activity of fractions F1–F4, CC_{10} of each fraction was determined in order to maintain 90% of cell viability for the anti-inflammatory activity. As depicted in Table 1, the macrophage J774 was less sensitive to F1 (12.63 μg/mL) compared to F2 (8.1 μg/mL) and F4 (8.8 μg/mL), which in turn were less cytotoxic than F3 (4.7 μg/mL).

The cells were exposed to each fraction (at a concentration approximating the CC_{10} value) and then activated with LPS for 24 h.

TABLE 1 Cytotoxicity of F1–F4 on murine J774 macrophages cell line

Fractions	CC_{10} (μg/mL)[a] Macrophages
F1	12.63 ± 6.60
F2	8.1 ± 3.39
F3	4.7 ± 1.83
F4	8.8 ± 1.53

[a]Resazurin viability assay was performed in order to obtain concentrations to maintain 90% of cell viability.

Thereafter, NO and TNF-α were then measured in the supernatants of macrophages. F1–F4 showed strong ability to inhibit NO and TNF-α release from activated macrophages (Figure 1). There was no significant difference among fractions, neither for NO nor TNF-α analysis, however, all fractions were able to significantly inhibit these inflammatory mediators in LPS-induced macrophages ($p < 0.01$ and $p < 0.001$).

3.1.2 | Antiparasitic activity

Fractions F1–F4 were further assayed on intracellular amastigotes of *T. cruzi* and *L. amazonensis* (Table 2). THP-1 cells were used as a host for the parasites. While F1, F3 and F4 displayed significant antitrypanosomal activity with IC_{50} values of 3.94, 3.58 and 3.82 μg/mL, respectively, with good selectivity towards THP-1 cells, F2 showed a weak effect (24.22 μg/mL) on the same parasite with a very low selectivity.

In addition, F1, F3 and F4 showed the most promising antileishmanial effect with IC_{50} at 8.08, 7.15 and 8.23 μg/mL, respectively, while F2 was weakly active (27.73 μg/mL). However, F1 and F4 displayed similar selectivity on the host cells (7.30 and 7.69, respectively)

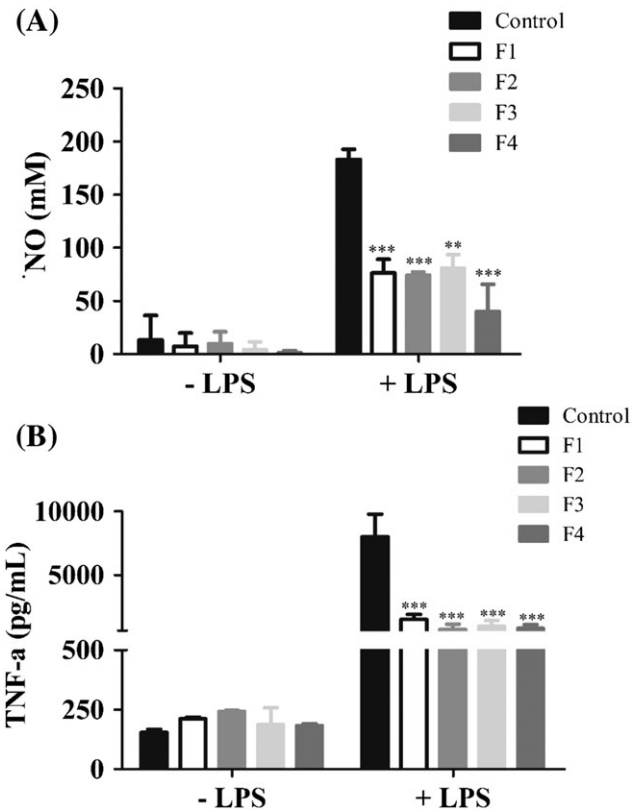

FIGURE 1 Cytokine release from activated macrophages. (A) •NO determination and (B) TNF-α in the supernatants of macrophages J774 with or without lipopolysaccharide (LPS) (10 μg/mL) in the presence of fractions at the concentrations 12 μg/mL (F1), 8 μg/mL (F2), 5 μg/mL (F3), and 9 μg/mL (F4). Data expressed as mean ± standard deviation of three experiments. One-way analysis of variance followed by Dunnett's multiple comparisons test was used for the statistical significance. $^{**}p < 0.01$, $^{***}p < 0.001$ compared with control group LPS+

TABLE 2 Inhibition effect of the resin fractions against *Trypanosoma cruzi* and *Leishmania amazonensis* and their selectivity index (SI) towards THP-1 cells

Fractions	*T. cruzi*		THP-1	*L. amazonensis*	
	IC_{50} (μg/mL)	SI	CC_{50} (μg/mL)	IC_{50} (μg/mL)	SI
F1	3.94 ± 0.43	14.97	58.99 ± 2.07	8.08 ± 1.64	7.30
F2	24.22 ± 1.08	2.93	70.99 ± 2.55	27.73 ± 3.41	2.56
F3	3.58 ± 0.31	24.55	87.89 ± 6.27	7.15 ± 1.60	12.29
F4	3.82 ± 0.33	16.57	63.32 ± 6.18	8.23 ± 1.20	7.69
α-Amyrin	NA	—	—	NA	—
α-Amyrone	NA	—	—	NA	—
11-Oxo-α-amyrin	8.67 ± 0.55	3.52	30.53 ± 0.90	11.6 ± 2.68	2.63
11-Oxo-α-amyrone	16.76 ± 0.76	8.40	140.8 ± 5.56	19.43 ± 2.28	7.24
Benznidazole	2.65 ± 0.08	>49.06	>130	—	—
Amphotericin B	—	—	25.74 ± 0.91	0.13 ± 0.02	198

Note: NA, not available.

while F3 and F2 showed the highest (12.29) and the lowest (2.56) selectivity, respectively.

An attempt to isolate single pure compounds in order to compare their bioactivity with the fractions led to α-amyrin. The metabolite was further oxidised by using three different reaction conditions (Figure 2) affording α-amyrone, 11-oxo-α-amyrone, and 11-oxo-α-amyrin. These four triterpenes were evaluated against both parasites among them, only 11-oxo-α-amyrone, and 11-oxo-α-amyrin revealed, respectively, IC_{50} at 16.76 and 8.67 μg/mL against *T. cruzi*. Moreover, both also showed effects on *L. amazonensis* with IC_{50} at 19.42 and 11.6 μg/mL, respectively.

3.2 | Chemistry

3.2.1 | LC–MS analysis

Since F1–F4 revealed interesting biological activities, their chemical constituents (Table 3) were characterised by using the hyphenated technique UPLC-ESI-MS and MS/MS. These fractions were most sensitive to the positive ionisation mode and the base peak ionisation parameter was employed for the acquisition of the chromatogram (Figure 3).

LC–MS analysis of F3 showed the presence of 17 metabolites, which were further subjected to collision-induced dissociation (CID) by exposing each metabolite to accelerated argon atoms.

Fraction F3 at 4.53 min exhibited the base peak ion *m/z* 455.3518 produced by the thermal induced loss of H_3CCO_2H (60 Da) from *m/z* 515.3730. The molecular formula $[C_{32}H_{50}O_5 + H]^+$ was then deduced for this metabolite which gave in its tandem mass (Figure S5) *m/z* 455.3518 $[M\text{-}AcOH\ (60\ Da) + H]^+$ which in turn eliminated H_2O (18 Da) and HCO_2H (46 Da) to produce *m/z* 437.3442 and *m/z* 409.3488, respectively. Assuming that the ionisation occurred on the OH group attached to ring E, the decalin ion formed from the retro-Diels–Alder (RDA) opening of ring C could either lead to *m/z* 203.1775 or to *m/z* 201.1653 after losing [H_2O (18 Da); CO_2

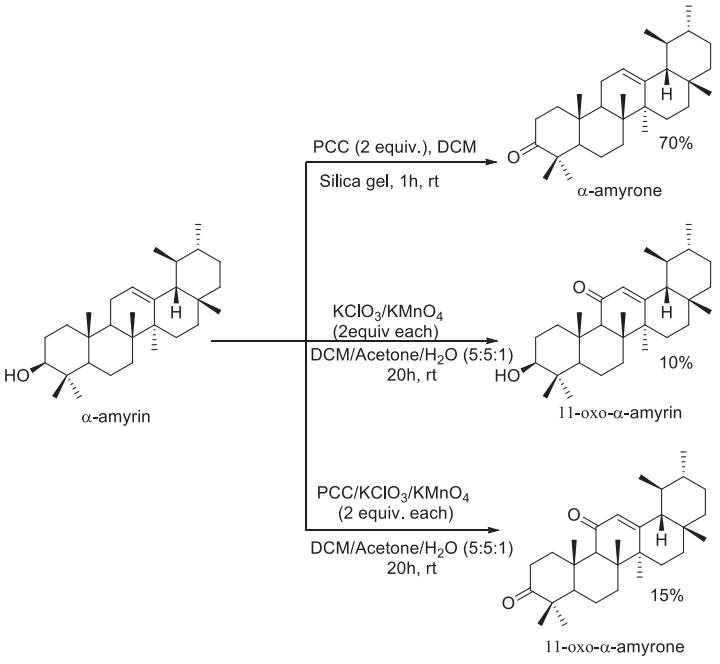

FIGURE 2 Preparation of derivatives related to α-amyrin

TABLE 3 Chemical profile of the *Cola nitida* resin fractions (F1–F4)

tR (Min)	Experimental mass (m/z)	Theorical mass (m/z)	Molecular formular	Fragments	Structure proposal	Fractions			
						F1	F2	F3	F4
4.53	455.3519/ 515.3730	455.3525[M-H_3CCO_2H + H]$^+$ /515.3736 [M + H]$^+$	$C_{30}H_{46}O_3$/ $C_{32}H_{50}O_5$	437.3442, 425.3455, 419.3270, 409.3488, 343.2635, 313.2548, 311.2383, 295.2458, 283.2469, 257.1937, 251.1651, 245.1920, 215.1821, 203.1775, 201.1653, 189.1643, 187.1501, 177.1674, 175.1507, 173.1347, 163.1489, 161.1333, 159.1199, 149.1355, 147.1169, 135.1182, 133.1028, 121.1030, 109.1031	Rubiprasin C or 3-i-acetyl pomolic acid			p	p
5.67	425.3792	425.3783 [M + H]$^+$	$C_{30}H_{48}O$	407.3693, 271.2441, 245.2273, 221.1935, 217.1968, 203.1804, 191.1808, 161.1359, 147.1194, 135.1182, 133.1028, 109.1031	Olean-12(13),15(16)-dien-3β-ol			p	p
6.33	457.3659	457.3683 [M + H]$^+$	$C_{30}H_{48}O_3$	439.3566, 421.3522, 411.3664, 393.3505, 343.2673, 313.2548, 295.2423, 259.2081, 247.2072, 241.1959, 229.1971, 215.1791, 187.1501, 173.1347, 159.1173, 135.1182, 121.1007, 109.1031	Oleanolic acid				p
6.51	425.3750	425.3783 [M + H]$^+$	$C_{30}H_{48}O$	407.3651, 311.2744, 271.2441, 217.1938, 203.1804, 191.1808, 175.1480, 147.1169, 133.1028, 123.1165, 109.1031	3-Hydroxy-urs-12,15-diene	p	p	p	p
6.66	909.6996	909.6972 [2 M + H]$^+$	$C_{30}H_{46}O_3$	437.3442, 419.3312, 409.3447, 369.2801, 313.2548, 311.2383, 295.2458, 257.1937, 245.1920, 201.1653, 203.1833, 189.1643, 187.1501, 159.1501, 133.1028, 109.1031	3β-Hydroxyurs-12,18-dien-28-oic acid or micromeric acid or 3β-hydroxyurs-12,19(29)-dien-28-oic acid		p	p	p
6.84	457.3659	457.3682 [M + H]$^+$	$C_{30}H_{48}O_3$	439.3609, 421.3522, 393.3505, 343.2635, 313.2584, 295.2423, 269.2303, 255.2132, 229.1971, 201.1653, 187.1501, 159.1173, 109.1031	Ursolic acid			p	p
6.92	443.3867	443.3889 [M + H]$^+$	$C_{30}H_{50}O_2$	425.3792, 407.3651, 315.2705, 297.2593, 259.2048, 247.2072, 243.2106, 229.1971, 215.1821, 187.1473 175.1507, 161.1333, 149.1355, 135.1182, 123.1182, 109.1031	Erythrodiol			p	p
7.14	427.3936	427.3940 [M + H]$^+$	$C_{30}H_{50}O$	409.3820, 299.2760, 271.2441, 229.1971, 217.1968, 191.1808, 189.1643, 163.1489, 149.1330, 137.1321, 135.1182, 123.1188, 121.1030, 109.1009	β-Amyrin			p	p
7.39	441.3737	441.3733 [M + H]$^+$	$C_{30}H_{48}O_2$		Dehydrouvaol			p	

(Continues)

TABLE 3 (Continued)

tR (Min)	Experimental mass (m/z)	Theorical mass (m/z)	Molecular formular	Fragments	Structure proposal	Fractions			
						F1	F2	F3	F4
				423.3654, 405.3533, 315.2705, 297.2593, 287.2397, 269.2303, 259.2048, 247.2072, 241.1991, 229.1971, 215.1821, 201.1682, 189.1643, 175.1507, 161.1333, 149.1355, 135.1182, 109.1031					
7.47	427.3936	427.3940 $[M + H]^+$	$C_{30}H_{50}O$	409.3820, 299.2760, 271.2441, 229.1971, 217.1968, 191.1808, 189.1643, 163.1489, 149.1330, 137.1321, 123.1188, 121.1030, 109.1009	α-Amyrin				p
7.65	441.3737	441.3733 $[M + H]^+$	$C_{30}H_{48}O_2$	423.3654, 405.3533, 315.2705, 297.2593, 259.2048, 247.2072, 241.1991, 229.1971, 215.1821, 189.1671, 177.1674, 161.1359, 149.1355, 135.1182, 121.1030, 109.1031	Related to dehydrouvaol		p	p	p
7.72	443.3867	443.3889 $[M + H]^+$	$C_{30}H_{50}O_2$	425.3792, 407.3651, 315.2705, 297.2593, 259.2048, 247.2072, 243.2106, 229.1971, 215.1821, 187.1473 175.1507, 161.1333, 149.1355, 123.1182, 109.1031	Uvaol				p
7.94	485.3981	485.3995 $[M + H]^+$	$C_{32}H_{52}O_3$	425.3750, 407.3693, 297.2628, 235.2115, 217.1968, 205.1968, 191.1808, 177.1647, 163.1489, 149.1330, 133.1028, 121.1030, 109.1031	3β-Acetoxy-28-hydroxy-urs-12-ene or 3-*O*-acetyl-erythrodiol		p		
8.02	499.3794	499.3787 $[M + H]^+$	$C_{32}H_{50}O_4$	439.3566, 355.2642, 343,2635, 297.2593, 241.1959, 229.1971, 217.1968, 203.1804, 201.1653, 191.1808, 189.1643, 187.1501, 135.1182, 121.1007, 109.1009	Oleanolic acid 3-acetate	p	p	p	
8.27	467.3878	467.3889 $[M + H]^+$	$C_{32}H_{50}O_2$	407.3651, 323.2731, 311.2744, 297.2593, 283.2434, 271.2441, 269.2303 217.1968, 203.1804, 191.1808, 189.1643, 161.1333, 147.1169, 133.1028, 109.1009	Ursa-12,20(30)-dien-3α-yl acetate or urs-12,19(29)-dien-3β-yl acetate or gigantursenyl acetate A	p	p	p	
8.38	499.3794	499.3787 $[M + H]^+$	$C_{32}H_{50}O_4$	439.3566, 421.3480, 405.3533, 393.3505, 313.2584, 297.2593, 295.2423, 247.2072, 241.1959, 229.1971, 203.1804, 191.1808, 189.1643, 161.1359, 147.1169, 135.1182, 121.1007, 109.1009	3β-*O*-Acetylursolic acid	p		p	
8.57	439.3609	439.3576 $[M + H]^+$	$C_{30}H_{46}O_2$	421.3480, 403.3424, 313.2511, 295.2423, 287.2397, 269.2303,	—				p

(Continues)

TABLE 3 (Continued)

tR (Min)	Experimental mass (m/z)	Theorical mass (m/z)	Molecular formular	Fragments	Structure proposal	Fractions F1	F2	F3	F4
				241.1991, 227.1789, 217.1998, 213.1679, 203.1804, 201.1653, 187.1501, 173.1347, 161.1333, 149.1355, 135.1182, 127.1127, 123.1188, 109.1009					
8.68	423.3612	423.3627 $[M + H]^+$	$C_{30}H_{46}O$	405.3533, 297.2558, 269.2303, 255.2132, 241.1959, 229.1971, 201.1653, 189.1643, 187.1501, 149.1355, 135.1182, 121.1030, 109.1031	Olean-9(11),12-dien-3-one			p	
8.93	441.3737	441.3733 $[M + H]^+$	$C_{30}H_{48}O_2$	423.3612, 405.3533, 297.2558, 269.2303, 255.2132, 241.1959, 229.1971, 201.1653, 189.1643, 187.1501, 149.1355, 135.1182, 121.1030, 109.1031	Related to dehydrouvaol	p	p	p	
9.48	423.3612	423.3627 $[M + H]^+$	$C_{30}H_{46}O$	405.3533, 297.2558, 269.2303, 255.2132, 241.1959, 229.1971, 201.1653, 189.1643, 187.1501, 149.1355, 135.1182, 121.1030, 109.1031	Ursa-9(11),12-dien-3-one			p	
12.60	409.3820	409.3820 $[M + H]^+$	$C_{30}H_{48}$	299.2725, 271.2441, 257.2265, 243.2138, 231.2140, 217.1968, 205.1939, 203.1804, 191.1808, 163.1489, 149.1330, 135.1182, 123.1188, 109.1009	Olean-11,13(18)-diene	p		p	p
13.19	409.3820	409.3820 $[M + H]^+$	$C_{30}H_{48}$	-	Related to olean-11,13(18)-diene			p	p
13.78	409.3820	409.3820 $[M + H]^+$	$C_{30}H_{48}$	313.2910, 285.2605, 259.2443, 257.2298, 231.2109, 203.1833, 177.1647, 149.1330, 137.1345, 123.1188, 109.1031	Related to olean-11,13(18)-diene	p	p	p	p

(44 Da)] or [H_2O (18 Da); HCO_2H (46 Da)], respectively. A careful search in the literature of the molecular formula aforementioned led to rubiprasin C or 3-*O*-acetyl pomolic acid structures. These compounds are two metabolites differing only by the position of the Me-29, which could be located either at C-19 (ursane) or C-20 (oleanane).[19] However, the daughter ions *m/z* 313.2548, and *m/z* 311.2383 (Figure 4) permitted to assign 3-*O*-acetyl pomolic acid as structure.

The ion *m/z* 425.3792 $[C_{30}H_{48}O + H]^+$ (5.67 min) gave a daughter ion *m/z* 407.3693 after losing a molecule of H_2O (18 Da). This ion further produced the fragment *m/z* 191.1808 by RDA ring C opening. Application of the charge-driven concerted reaction (R1) concept on *m/z* 407.3693 led to an intermediate with opened rings A–C. This latter underwent a [1,5]-elimination at the position indicated in Figure S5 to afford *m/z* 203.1804 and *m/z* 271.2441; More fragments illustrated in Figure S5 allowed the assignment of *m/z* 425.3792 structure as anhydrosophoradiol. Similar fragmentation pattern was observed for the metabolite detected at 6.51 min with the same mass value *m/z* 425.3750 $[C_{30}H_{48}O + H]^+$. The diagnostic of its MS data suggested this compound to be closely related to the one identified earlier and 3-hydroxy-urs-12,15-diene was proposed as the presumable structure.

The ion *m/z* 909.6996 detected at 6.66 min corresponded to a cluster species with the molecular formula $[2C_{30}H_{46}O_3 + H]^+$. It afforded in its MS^2 spectrum, ions at *m/z* 437.3442 and *m/z* 419.3312 after losing H_2O (18 Da) and $2H_2O$ (36 Da), respectively. This parent ion further underwent a decarboxylation (HCO_2H, 46 Da) to give *m/z* 409.3447; three ion species (Figure S6) were found with the mass *m/z* 437.3442 among them, one with the positive charge on the carbonyl carbon. As depicted in Figure S6, this latter underwent a ring E opening with the elimination of a hydrocarbon portion to produce *m/z* 313.2526 which in turn lost H_2O (18 Da) to afford *m/z* 295.2558; Moreover, if the ionisation occurred in ring E, the RDA opening of ring C gave a decalin moiety composed of rings D and E. The ions *m/z* 203.1833 and *m/z* 201.1653 were formed out of this decalin after the decarboxylation

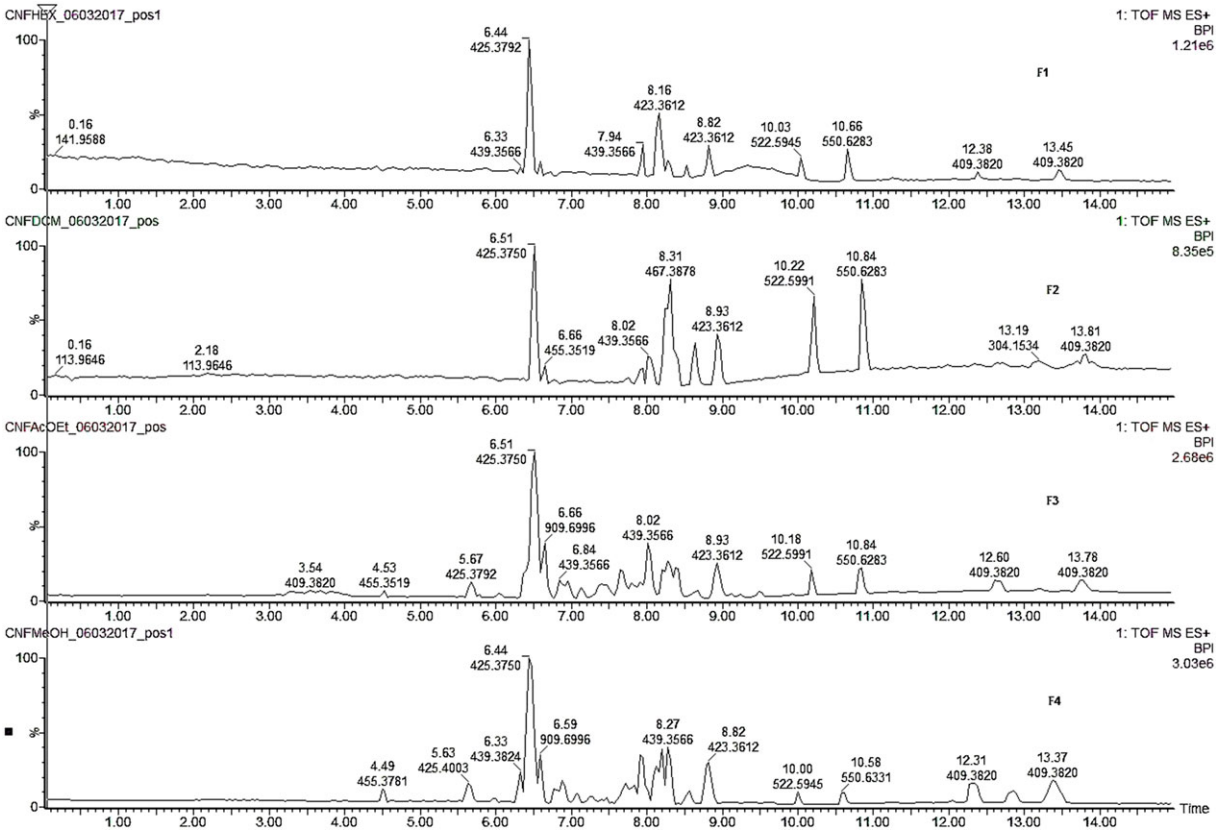

FIGURE 3 LC-ESI-MS of F1–F4 in the positive mode ionisation

CO_2 (44 Da) and HCO_2H (46 Da), respectively. The aforementioned information conducted to a structure related to 3β-hydroxyurs-12,18-dien-28-oic acid or micromeric acid or 3β-hydroxyurs-12,19(29)-dien-28-oic acid. These three metabolites differ from each other by the position of the double bond which could not be well established from the ions formed.

The metabolite at *m/z* 457.3659 $[C_{30}H_{48}O_3 + H]^+$ [retention time (tR) 6.84 min] exhibited in its MS^2 spectrum fragment ions *m/z* 439.3609, *m/z* 421.3522 and *m/z* 393.3505 formed after it lost H_2O, $2H_2O$ and (H_2O, HCO_2H), respectively. The fragmentation proposal led to two ions with the mass value *m/z* 439.3609 among them, one bearing the charge on the carbonyl carbon. Because that position of the charge, its migration triggered the opening of rings D and E to afford *m/z* 313.2584 which in turn lost H_2O to give *m/z* 295.2423 (Figure S7); from the earlier mentioned data, the structure of oleanolic acid was assigned. A second compound with the same mass value *m/z* 457.3659 $[C_{30}H_{48}O_3 + H]^+$ was detected (tR 6.33 min) in F4 and the structure of ursolic acid was attributed. However, their fragmentation pattern proposal displayed features similar to those previously reported.[20,21]

The compound *m/z* 443.3867 $[C_{30}H_{50}O_2 + H]^+$ (6.92 min) displayed in its MS^2 spectrum, peaks corresponding to the loss of H_2O and $2H_2O$ at *m/z* 425.3792 and *m/z* 407.3651, respectively. Ring C in this latter ion opened in a RDA manner to afford an ion fragment, which in turn produced *m/z* 175.1505 after losing acetylene. The ion *m/z* 425.3792 containing the primary carbocation afforded *m/z* 315.2705 after the opening of rings D and E and the loss of a hydrocarbon moiety (Figure S8). Furthermore, *m/z* 297.2593 was lighter of 18 Da from *m/z* 315.2705 presumably due to the loss of H_2O. The combination of the earlier information led to the structure of erythrodiol.[21] A compound was also found in the LC–MS analysis of F4 with almost the same MS^2 behaviour. The structure of uvaol, an ursane type was proposed and no evidence in its fragmentation pattern permitted to distinguish its structure from erythrodiol. However, the daughter ions obtained matched those previously reported.[22]

The precursor *m/z* 427.3936 $[C_{30}H_{50}O + H]^+$ (7.14 min) furnished in its MS^2 spectrum a fragment ion *m/z* 409.3820 resulting from the loss of H_2O (18 Da). This fragment further underwent a RDA opening of ring C to produce *m/z* 191.1808. It also went through a charge-driven concerted reaction leading to the opening of rings A, B, and C; the intermediate ion lost different hydrocarbon portions as depicted in Figure S9 to afford *m/z* 189.1643 and *m/z* 271.2441; this latter in turn gave *m/z* 229.1971 after eliminating propene. Another fragment was found at *m/z* 217.1968 when the ionisation occurred on the olefinic bond of *m/z* 427.3936 forming a tertiary carbocation. This ion position triggered the opening of ring C and produced *m/z* 217.1968 after eliminating the fused rings D and E as well as H_2O. Since none of these fragments allowed to univocally identify the metabolite at *m/z* 427.3936, two structures namely α- and β-amyrin were found in the literature for this metabolite. By comparing this data with those previously reported,[21] *m/z* 427.3936 was assigned as β-amyrin. Another metabolite with the same elemental composition was detected in F4 at 7.47 min. Its tandem mass analysis revealed fragmentation pattern similar to *m/z* 427.3936 $[C_{30}H_{50}O + H]^+$ (7.14 min) found in F3 and the structure of α-amyrin was proposed.

The tandem mass analysis of *m/z* 441.3737 $[C_{30}H_{48}O_2 + H]^+$ (tR 7.39 min) produced *m/z* 423.3654 and *m/z* 405.3533 from the

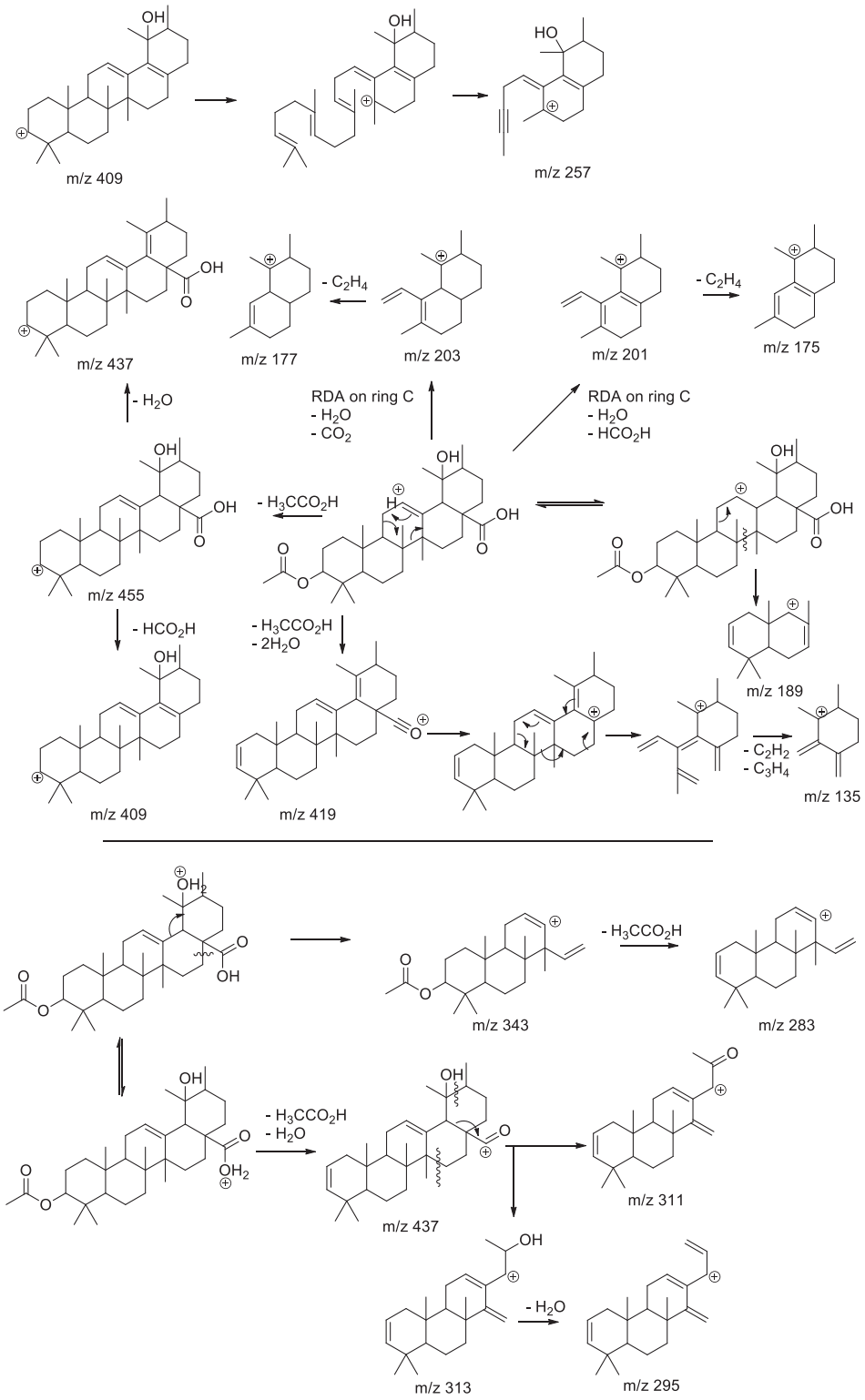

FIGURE 4 Proposal of *m/z* 515.3730 fragmentation pattern (4.53 min)

elimination of H_2O (18 Da) and $2H_2O$ (36 Da), respectively. Two ions were found with the mass value *m/z* 423.3654 among them, the one bearing a primary carbocation gave *m/z* 215.1821 through a RDA pathway on ring C; meanwhile, the charge migration via R1 in the same primary carbocation combined rings D and E. Furthermore, the loss of a hydrocarbon residue as shown in Figure S10 led to *m/z* 315.2705 which in turn afforded lighter fragments at *m/z* 297.2593, *m/z* 287.2397 and *m/z* 269.2303 after losing, respectively, H_2O, C_2H_4 (28 Da) and (H_2O and C_2H_4). The second ion *m/z* 423.3654 bearing a secondary carbocation could also undergo R1 through a supposed retro-biosynthesis pathway over three isoprenyl groups. The loss of hydrocarbon portions involved in rings A and B and MeOH (32 Da) via charge-remote elimination reaction (R2), gave *m/z* 287.2397 and *m/z* 241.1991; Moreover, when the ionisation occurred on the olefinic bond of *m/z* 441.3737, ring C opened through R1 and the intermediate formed lost MeOH (32 Da) to afford *m/z* 201.1682.

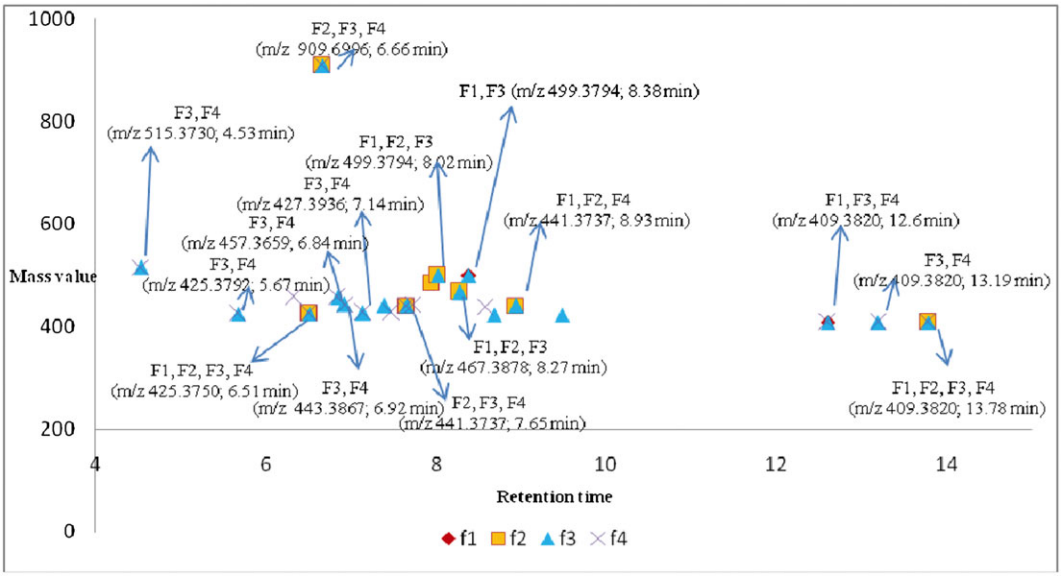

FIGURE 5 Correlation of F1–F4 based on their chemical composition [Colour figure can be viewed at wileyonlinelibrary.com]

This latter in turn eliminated C_2H_2 (26 Da) yielding *m/z* 175.1507. The combination of the foregoing data allowed the identification of *m/z* 441.3737 as dehydrouvaol. Its isomers were also detected at 7.65 min and 8.93 with the same fragmentation pattern.

The peak at 8.02 min flanked with the mass value *m/z* 499.3794 $[C_{32}H_{50}O_4 + H]^+$ gave ions at *m/z* 439.3599, *m/z* 421.3480, and *m/z* 393.3546 representing fragments formed from the elimination of H_3CCO_2H (60 Da), [H_3CCO_2H and H_2O (78 Da)], and [H_3CCO_2H and HCO_2H] (106 Da), respectively (Figure S11). The precursor *m/z* 499.3794 further lost H_2O and the delocalisation of the positive charge in the ion product followed by the loss of the hydrocarbon moiety from rings D and E afforded *m/z* 343.2673; this ion, in turn, eliminated H_3CCO_2H (60 Da) and the resulting ion underwent an RDA opening of ring A to afford *m/z* 201.1653. The ion daughter *m/z* 439.3599 showed also a charge delocalisation (R1) followed by the opening of rings A–C in a retro-biosynthetic manner. Moreover, the intermediate formed, lost C_6H_{12} (84 Da), and [$C_{11}H_{20}$ and HCO_2H] (198 Da) to furnish *m/z* 355.2642 and *m/z* 241.1959, respectively. The foregoing data in conjunction with additional ions illustrated in Figure S11 led to the structure of oleanolic acid 3-acetate. Another metabolite was detected at 8.38 min with the same mass value, which gave almost the similar fragmentation pattern and 3β-*O*-acetylursolic acid was assigned as its structure.

The ion *m/z* 467.3878 $[C_{32}H_{50}O_2 + H]^+$ was the mass value of the metabolite detected at 8.31 min which provided on its tandem mass spectrum the fragment *m/z* 407.3651 after losing H_3CCO_2H (60 Da). This ion daughter produced in turn *m/z* 191.1808 after a RDA opening of ring C. Rings A–C opened while the charge delocalisation occurred and the intermediate formed lost two isoprenyl units ($C_{10}H_{16}$, 136 Da) to afford *m/z* 271.2441; *m/z* 203.1804 resulted from *m/z* 271.2441 after another isoprenyl (68 Da) unit loss. On the basis, of the information shown in Figure S12, the structure was established as ursa-12,20(30)-dien-3α-yl acetate or urs-12,19(29)-dien-3β-yl acetate.

Two ions were obtained at 8.68 min and 9.48 min with similar mass values *m/z* 423.3612 corresponding to $[C_{30}H_{46}O + H]^+$. Both precursors afforded similar MS^2 fragments. The ion daughter *m/z* 405.3533 was produced after the precursor lost H_2O (18 Da). As showed in Figure S13, rings A–C in this fragment (*m/z* 405.3533) further opened due to the delocalisation of the positive charge and the loss of different hydrocarbon moieties conducted to the formation of *m/z* 255.2132, *m/z* 297.2558, *m/z* 269.2303, and *m/z* 229.1971 (Table 3); additional fragmentation displayed in Figure S13 enabled the identification of these metabolites as olean-9 (11),12-dien-3-one and ursa-9 (11),12-dien-3-one.

Two last metabolites were detected at 12.6 min and 13.78 min with identical mass values *m/z* 409.3820, which corresponded to $[C_{30}H_{48} + H]^+$. Based on fragmentation pattern shown in Figure S14, the earlier detected metabolite was identified as olean-11,13(18)-diene and the second on as its related derivative.

LC–MS analysis of fraction F2 displayed a unique metabolite difference from those found in F3. So, the precursor *m/z* 485.3981 $[C_{32}H_{52}O_3 + H]^+$ furnished *m/z* 425.3792 and 407.3651 after losing H_3CCO_2H (60 Da) and [H_3CCO_2H and H_2O (78 Da)], respectively. A RDA rearrangement occurred in ring C of *m/z* 425.3981 to afford *m/z* 191.1808; *m/z* 297.2593 was formed from *m/z* 407.3651 which underwent a charge migration and a loss of a hydrocarbon moiety. The precursor *m/z* 485.3981 produced through a RDA rearrangement in ring C the ion *m/z* 235.2115 which in turn lost H_2O (18 Da) and [H_2O and C_2H_2 (46 Da)] to give *m/z* 217.1968 and 191.1808, respectively. Assuming that the ionisation occurred on the olefinic carbons, the first carbocation in C-12 could trigger a charge delocalisation leading to the opening of ring C. The obtained intermediate lost CH_3OH (32 Da) to afford *m/z* 205.1968; this latter in turn eliminated C_2H_4 (28 Da) to give *m/z* 177.1647. Moreover, the carbocation in C-13 could also produce *m/z* 217.1968 as depicted in Figure S15. From the data outlined earlier, the structure was assigned as 3β-acetoxy-28-hydroxy-urs-12-ene or 3-*O*-acetyl-erythrodiol.

LC–MS of F1 revealed metabolites already identified in F3 while the F4 analysis showed exclusive compounds such as oleanolic acid, α-amyrin, uvaol and an unidentified metabolite (Table 3). Their structures were established using the fragmentation pattern compared to the data reported in the literature.[22]

4 | DISCUSSION

4.1 | Anti-inflammatory study

Figure 5 showed that F3 contains three components including dehydrouvaol, olean-9 (11),12-dien-3-one and ursa-9 (11),12-dien-3-one which were not detected in F1, F2, and F4. These metabolites might be responsible for its strong cytotoxicity on J774. Moreover, LC–MS analysis of F1 revealed the presence of fewer constituent than the others and its metabolites were also detected in other fractions. Thus, its lowest cytotoxicity suggested that a part of F2 and F4 compounds might strongly affect the macrophage viability.

Despite their different cytotoxic effect fractions F1-F4 almost equally showed strong inhibition of NO and TNF-α regardless their different composition. The identified constituents are mainly pentacyclic triterpenes related to α- and β-amyrin. Oleanolic acid as well as its derivatives were previously reported to inhibit NO production by LPS-activated RAW 264.7 and J774A.1 cells.[23] More importantly, oleanolic acid and its 3-oxo- and 3-oxo-28-methyl ester derivatives previously revealed almost the same inhibitory effect.[23] This suggested that structural differences such as oxidised functions or an increase of the double bond equivalent observed within the constituents do not highly change the anti-inflammatory activity from a fraction to another. The prepared triterpenes were not enough to be evaluated for their anti-inflammatory activity and compared their effects to those of the fractions. However, previous studies on anti-inflammatory effects of α-amyrin, α-amyrone, 11-oxo-α-amyrone, and 11-oxo-α-amyrin reported the ability of these metabolites to reduce the level of NO and TNF-α production.[24-26]

4.2 | Antiparasitic activity

Interestingly, F1, F3, and F4 also showed close antitrypanosomal activity. Figure 5 revealed that the seven constituents of F1 are present in other fractions. However, only four of these metabolites including oleanolic acid 3-acetate, olean-11,13(18)-diene, and two compounds related to dehydrouvaol and to olean-11,13(18)-diene were found in F3 and F4. The observation suggested that the obtained antitrypanosomal activity and the similarity depended on the presence of these four metabolites. Meanwhile, F2 was eight-fold less active than the other fractions although it contained seven metabolites similar to those found among the F1, F3 and F4 constituents. However, this fraction also contained the metabolite *m/z* 467.3878 (ursa-12,20(30)-dien-3α-yl acetate or urs-12,19(29)-dien-3β-yl acetate or gigantursenyl acetate A as the second major component which could interfere in its antitrypanosomal action.

Features similar to those observed for antitrypanosomal activity, were also found in leishmanicidal activity. F1, F3 and F4 inhibited *L. amazonensis* with almost the same strength. However, the antileishmanial effect of F3 was lightly pronounced suggesting that the metabolites namely dehydrouvaol, olean-9 (11),12-dien-3-one, and ursa-9 (11),12-dien-3-one only present in F3 might be responsible for the little improvement of its activity. Fraction F2 was also weakly active on this parasite and three-fold less potent than the others presumably because of its chemical composition as outlined earlier.

Except for F2, the other fractions showed antiprotozoal activity with moderate toxicity on the host THP-1 cells. The predominance of the compound *m/z* 467.3878 in F2 identified as ursa-12,20(30)-dien-3α-yl acetate or urs-12,19(29)-dien-3β-yl acetate or gigantursenyl acetate A presumably affected the THP-1 cells viability.

In general, the antiparasitic activity of pentacyclic triterpenes and enriched pentacyclic triterpenes extracts is well documented. So, oleanane and ursane derived secondary metabolites previously revealed moderate to significant effect against both parasites.[27] However, except for α-amyrin and α-amyrone, the dioxygenated derivatives were active against the parasites and their potencies were lower than those obtained for the fractions. This suggested a possible synergistic action of the constituents in the most active fractions or eventually the presence of a principle active.

The resin collected from *C. nitida* was separated into four fractions (F1–F4) because of its sticky behaviour. The obtained fractions were evaluated for their anti-inflammatory activity, from which a similar potential was observed for all. It was noted that CO, OH and olefinic functions distributed on a pentacyclic triterpene skeleton do no create a real difference among the anti-inflammatory potency of the fractions. On the basis of the obtained results, the *C. nitida* resin might be used to develop an anti-inflammatory phytomedicine. Moreover, the fractions were also evaluated for their antiparasitic effect. Fractions F1, F3, and F4 revealed interesting antiparasitic effect on intracellular *L. amazonensis* and *T. cruzi* amastigotes. The fractions antiparasitic activities were better than those of the hemisynthetic triterpenes (prepared from three different oxidation reactions of α-amyrin) and α-amyrin. This later result suggested a synergistic contribution of the fraction constituents. It also suggested that a mixture of oleanane and ursane triterpenes can be used to prepare a low toxic antiparasitic drug. Overall, whether this plant secretion has an effect on spirit or not, the herein results revealed this resin as a great source of biological active triterpenes.

ACKNOWLEDGEMENTS

The authors would like to thank CNPq (Conselho Nacional de Desenvolvimento Científico e Tecnológico) and CAPES (Coordenação de Aperfeiçoamento de Pessoal de Nível Superior) for their financial support. This work is a collaborative production of M.S, M.W.B, and L.P.S, members of the Research Network Natural Products against Neglected Diseases (ResNetNPND). L.P.S would like to thank M. Pierre Seumen for the resin collection.

ORCID

Louis P. Sandjo http://orcid.org/0000-0001-5840-7733

REFERENCES

1. Davies E. Mummy mania. *Chemistry World*. 2011;8(2):48-51.
2. Langenheim JH. *Plant Resins Chemistry. Evolution, Ecology, and Ethnobotany Timber*. Cambridge, MA: Portland Press; 2003:23-40.
3. Abdel-Maksouda G, El-Aminb A-R. A review on the materials used during the mummification processes in ancient Egypt. *Mediterr Archaeol Archaeometry*. 2011;11:129-150.
4. Jura-Morawiec J, Tulik M. Dragon's blood secretion and its ecological significance. *Chem*. 2016;26:101-105.

5. Messer A, McCormick K, Hagedorn SHH, Tumbel F, Meinwald J. Defensive role of tropical tree resins: Antitermitic sesquiterpenes from southeast Asian Dipterocarpaceae. *J Chem Ecol*. 1990;16:3333-3352.
6. Termentzi A, Fokialakis N, Skaltsounis AL. Natural resins and bioactive natural products thereof as potential anitimicrobial agents. *Curr Pharm Des*. 2011;17:1267-1290.
7. Umoh IO, Emmanuel OA, Nna VU. Aqueous seed extract of *Cola nitida* rubra reduces serum reproductive hormone concentrations and sperm count in adult male albino Wistar rats. *Niger Med J*. 2014;55:456-459.
8. Marquez-Martin A, De La Puerta R, Fernandez-Arche A, Ruiz-Gutierrez V, Yaqoob P. Modulation of cytokine secretion by pentacyclic triterpenes from olive pomace oil in human mononuclear cells. *Cytokine*. 2006;36:211-217.
9. Huang J, Wang Y, Li C, Wang X, He X. Triterpenes isolated from acorns of *Quercus serrata* var. brevipetiolata exert anti-inflammatory activity. *Ind Crops Prod*. 2016;91:302-309.
10. Peláez GLM, Sierra JA, Alzate F, Holzgrabe U, Ramirez-Pineda JR. Pentacyclic triterpenes from *Cecropia telenitida* with immunomodulatory activity on dendritic cells. *Braz J Pharmacog*. 2013;23:754-761.
11. Zhou J, Wei X-h, F-y C, et al. Anti-inflammatory pentacyclic triterpenes from the stems of *Euonymus carnosus*. *Fitoterapia*. 2017;118:21-26.
12. Ahmed SA, Gogal RM Jr, Walsh JE. A new rapid and simple non-radioactive assay to monitor and determine the proliferation of lymphocytes: an alternative to [^{3}H] thymidine incorporation assay. *J Immunol*. 1994;170:211-224.
13. Herath HM, Takano-Ishikawa Y, Yamaki K. Inhibitory effect of some flavonoids on tumor necrosis factor-alpha production in lipopolysaccharide-stimulated mouse macrophage cell line J774.1. *J Med Food*. 2003;6(4):365-370.
14. Griess P. Bemerkungen zu der Abhandlung der HH. Weselsky und Benedikt "Ueber einige Azoverbindungen". *Ber Dtsch Chem Ges*. 1879;12:426-428.
15. Schwende H, Fitzke E, Ambs P, Dieter P. Differences in the state of differentiation of THP-1 cells induced by phorbol ester and 1,25-dihydroxyvitamin D3. *J Leukoc Biol*. 1996;59:555-561.
16. Buckner FS, Verlinde CL, La Flamme AC, Van Voorhis WC. Efficient technique for screening drugs for activity against *Trypanosoma cruzi* using parasites expressing β-galactoside. *Antimicrob Agents Chemother*. 1996;40:2592-2597.
17. Sieuwerts AM, Klijn JGM, Peters HA, Foekens JA. The MTT tetrazolium salt assay scrutinized: How to use this assay reliably to measure metabolic activity of cell cultures *in vitro* for the assessment of growth characteristics, IC_{50}-values and cell survival. *Clin Chem Lab Med*. 1995;33:813-824.
18. Van de Loosdrecht A, Nennie E, Ossenkoppele G, Beelen R, Langenhuijsen M. Cell mediated cytotoxicity against U 937 cells by human monocytes and macrophages in a modified colorimetric MTT assay. A methodological study. *J Immunol Methods*. 1991;141:15-22.
19. Li H, Yao W, Liu Q, et al. Application of UHPLC-ESI-Q-TOF-MS to identify multiple constituents in processed products of the herbal medicine *Ligustri Lucidi Fructus*. *Molecules*. 2017;22:689. https://doi.org/10.3390/molecules22050689
20. Jo H-J, Han JY, Hwang H-S, Choi YE. β-Amyrin synthase (EsBAS) and β-amyrin 28-oxidase (CYP716A244) in oleanane-type triterpene saponin biosynthesis in *Eleutherococcus senticosus*. *Phytochemistry*. 2017;135:53-63.
21. Gobo LA, Viana C, Lameira OA, de Carvalho LM. A liquid chromatography-atmospheric pressure photoionization tandem mass spectrometric (LC-APPI-MS/MS) method for the determination of triterpenoids in medicinal plant extracts. *J Mass Spectrom*. 2016;51:558-565.
22. McGhie TK, Hudault S, Lunken RCM, Christeller JT. Apple peels, from seven cultivars, have lipase-inhibitory activity and contain numerous ursenoic acids as identified by LC-ESI-QTOF-HR-MS. *J Agric Food Chem*. 2012;60:482-491.
23. Bhandari P, Patel NK, Gangwal RP, Sangamwar AT, Bhutani KK. Oleanolic acid analogs as NO, TNF-α and IL-1β inhibitors: Synthesis, biological evaluation and docking studies. *Bioorg Med Chem Lett*. 2014;24:4114-4119.
24. Chib R, Kumar M, Rizvi M, et al. Anti-inflammatory terpenoids from *Boswellia ovalifoliolata*. *RSC Adv*. 2014;4:8632-8637.
25. De Almeida PDO, de Boleti APA, Rüdiger AL, Lourenço GA, da Veiga Junior VF, Lima ES. Anti-inflammatory activity of triterpenes isolated from *Protium paniculatum* oil-resins. *J Evid Based Complement Altern Med*. 2015;2015. https://doi.org/10.1155/2015/293768
26. Folmer F, Dicato M, Diederich M. From the deepest sea shelf to the uppermost kitchen cabinet shelf: The quest for novel TNF-α inhibitors. *Curr Top Med Chem*. 2012;12:1392-1407.
27. Isah MB, Ibrahim MA, Mohammed A, Aliyu AB, Masola B, Coetzer THT. A systematic review of pentacyclic triterpenes and their derivatives as chemotherapeutic agents against tropical parasitic diseases. *Parasitology*. 2016;143:1219-1231.

SUPPORTING INFORMATION

Additional supporting information may be found online in the Supporting Information section at the end of the article.

The carbon NMR data of semi-synthetic compounds have been provided as additional supporting information as well as the fragmentation pattern of the identified compounds.

How to cite this article: Frankenberger L, Mora TD, de Siqueira CD, et al. UPLC-ESI-QTOF-MS^2 characterisation of *Cola nitida* resin fractions with inhibitory effects on NO and TNF-α released by LPS-activated J774 macrophage and on *Trypanosoma cruzi* and *Leishmania amazonensis*. *Phytochemical Analysis*. 2018;1-13. https://doi.org/10.1002/pca.2771